Two-photon Zeeman spectroscopy of terbium (III) elpasolites

A. J. Berry, R. G. Denning, and I. D. Morrison

Citation: The Journal of Chemical Physics **106**, 8967 (1997); doi: 10.1063/1.474010
View online: http://dx.doi.org/10.1063/1.474010
View Table of Contents: http://scitation.aip.org/content/aip/journal/jcp/106/22?ver=pdfcov
Published by the AIP Publishing

Two-photon Zeeman spectroscopy of terbium (III) elpasolites

A. J. Berry, R. G. Denning,[a] and I. D. Morrison
Inorganic Chemistry Laboratory, South Parks Road, Oxford, OX1 3QR, United Kingdom

(Received 5 February 1997; accepted 3 March 1997)

Polarised two-photon excitation (TPE) spectroscopy is a powerful technique for probing the energy levels of f-block elements at high symmetry sites because most pure electronic transitions are allowed by the selection rules. TPE in a magnetic field provides additional information, through the resolution of Zeeman components, evaluation of g-values, and the appearance of intensity in forbidden transitions. Here we present the selection rules and polarisation dependence for two-photon absorption at cubic sites, in a magnetic field. Polarised TPE spectra for the elpasolites Cs_2NaTbX_6 (X=F, Cl) are in excellent agreement with theory. The sensitivity of the second order Zeeman effect to the orientation of a cubic crystal relative to the magnetic field is illustrated, together with successful modelling of the Zeeman interaction for a number of multiplets. © *1997 American Institute of Physics.* [S0021-9606(97)00122-0]

I. INTRODUCTION

The cubic Cs_2NaLnX_6 (X=F, Cl) elpasolite lattice (space group $Fm3m$) provides a perfectly octahedral lanthanide site,[1] and is stable to liquid helium temperatures for most trivalent cations. The high site symmetry requires two one-electron crystal field and 32 two-electron correlation crystal field (CCF) parameters to model the f-electron-lattice interaction.[2,3] In this symmetry, one-photon f-f transitions are electric dipole forbidden, magnetic dipole transitions are rarely observed, and the absorption cross-section of vibronic transitions is low. Energy level data are therefore usually obtained from the emission spectrum, but this only locates the emitting levels and components of multiplets near the ground state. An empirical Hamiltonian for the chloride elpasolites has therefore been parameterised with data from an average of only 30 levels for each lanthanide.[4,5] Low symmetry sites such as those in $LaCl_3$ (C_{3h}) and LaF_3 (C_2) allow the identification of over 200 energy levels,[6,7] but the appropriate Hamiltonian requires up to 9 one-electron and 637 CCF parameters.

By contrast in two-photon spectroscopy, parity-conserving pure electronic transitions are allowed, and the spectra are usually free of phonon structure.[8,9] This allows numerous excited state energy levels to be identified in octahedral symmetry, creating a suitably large data set upon which to base an investigation of the CCF.[10] In two-photon excitation (TPE) spectroscopy the symmetry of the excited states may often be determined from polarisation data.[11] This is of particular value in cubic materials that are of course isotropic for one-photon processes.

Here we emphasise the additional value of TPE spectra in the assignment and characterisation of excited states, when the measurements are made in a magnetic field. We first develop selection rules and polarisation dependent expressions for two-photon intensity at an octahedral site in a magnetic field. Zeeman data are then presented for Cs_2NaTbX_6 (X=F, Cl) and compared with a theoretical model. Terbium(III) has a window of linear absorption transparency between 6 000 and 20 000 cm^{-1}, allowing non-resonant two-photon absorption to states up to ~40 000 cm^{-1}.

Two-photon spectra have previously been reported for the $^5D_4$ multiplet of Tb^{3+} in LaF_3 (Ref. 12) and for some levels of Tb^{3+} in $LiYF_4$ between 39 000 and 42 000 cm^{-1}.[13,14] The conjunction of one and two-photon data located 165 levels of Tb^{3+} in $LiYF_4$ up to 42 000 cm^1, however this includes two large gaps in which no observations were made.[13] The S_4 site symmetry requires five one-electron crystal field parameters, and although this Hamiltonian fits the data well, it is not clear to what extent the level assignments are unambiguous. The only detailed use of the Zeeman effect in two-photon lanthanide spectroscopy is in an analysis of the $^8S_{7/2}\rightarrow{}^6P_{7/2}$ region of $Gd(OH)_3$, where the Gd^{3+} ion is in a C_{3h} site.[15]

This paper establishes the methodology for analysing two-photon Zeeman spectra in a cubic site. Comprehensive energy level data on the fluoride, chloride, and bromide elpasolites of terbium(III), covering around 100 levels in each material, will be presented in due course. The broader objective is to identify the influence of the ligand chemical characteristics on the correlation crystal field.

II. EXPERIMENT

Two-photon excitation of Tb^{3+} is followed by rapid non-radiative decay to the $^5D_{4,3}$ multiplets, from which emission occurs to the ^7F_J manifold. The spectra were obtained by monitoring the $^5D_4\rightarrow{}^7F_J$ emission as a function of excitation energy. Emission was excited using a Q-switched Nd-YAG pumped dye laser, which could be Raman shifted in H_2. The laser frequency was determined to <1 cm^{-1} by simultaneously recording the opto-galvanic spectrum of an Ar discharge tube, as well as the transmission of an etalon with a free spectral range of 1.12 cm^{-1}. Luminescence was detected by an EMI 9813QB photomultiplier, LeCroy VV100B pulse preamplifier, and SR400 photon counter. The sample was mounted in a Thor Cryogenics magneto-optic

[a]Author to whom correspondence should be addressed.

cryostat, having a maximum field of 5.0 Tesla. The emission was first tightly focused onto a rotating chopper blade and then via bandpass filters onto the photomultiplier. The laser was fired by the chopper synchronisation output, delayed to a time ~1 ms prior to the point in the rotation cycle at which the blade opens the optical path to the detector. Because the luminescence lifetimes at 10 K are 9.5 ms for the chloride compound and 17.3 ms for the fluoride, the chopper prevents saturation of the detector by scattered laser light, but allows the detection of the majority of the luminescence. The emission was collected perpendicular to the excitation beam, and parallel to the magnetic field. When the polarisation of Zeeman components was not of interest, the excitation beam was depolarised by a birefringent quartz wedge.

Single crystals of Cs_2NaTbF_6 were grown by zone refinement, and those of $Cs_2NaTbCl_6$ by the Bridgeman method. Crystals were oriented by Laué back reflection, and faces were cut and polished perpendicular to {100}.

III. DISCUSSION

A. Selection rules

Two-photon transitions require two applications of the electric dipole operator. Its components can be written in spherical tensor notation,[16]

$$C_0^{(1)}=z/r, \quad C_{\pm 1}^{(1)}=\pm\frac{1}{\sqrt{2}}(x\pm iy)/r,$$

$$z=rC_0^{(1)}, \quad x=-\frac{r}{\sqrt{2}}(C_{+1}^{(1)}-C_{-1}^{(1)}),$$

$$y=\frac{ir}{\sqrt{2}}(C_{+1}^{(1)}+C_{-1}^{(1)}).$$

TPA intensity mechanisms for lanthanide f-f transitions have been discussed by Downer.[17] In an $LSJM_J$ basis the most general of these is a fourth order process, in which the transition moment connecting states $|g\rangle$ and $|f\rangle$ contains contributions of the form:

$$\sum_{j,m,n}\Delta E_j^{-1}\Delta E_m^{-1}\Delta E_n^{1}\langle g|C_{0,\pm 1}^{(1)}|j\rangle\langle j|C_{0,\pm 4}^{(k)}|m\rangle\langle m|\mathbf{L.S}|n\rangle \times\langle n|C_{0,\pm 1}^{(1)}|f\rangle. \quad (1)$$

In this expression the fourth and sixth rank tensor operators $C_{0,\pm 4}^{(k)}$ $(k=4,6)$ describe the crystal field perturbation in octahedral symmetry, and the spin-orbit operator **L.S** allows changes in the nominal spin multiplicity. Each application of the electric dipole operator, represented by the first rank tensors in equation (1), can change M_J by 0 or ± 1. The crystal field links states differing in M_J by 0 or ± 4, while **L.S** is diagonal in this quantum number.

In the experimental configuration, the magnetic field is parallel to [001], which we define as z, and the excitation beam propagates in the [010] or y direction, with its electric field vector in the xz plane. An experiment in which both photons are polarised parallel to the z axis (at 0° to the field) is denoted by the label zz. The non-zero elements of the electric dipole operator can then be represented by the tensor product $C_0^{(1)}C_0^{(1)}$, which conserves M_J. When combined with the crystalline field perturbation, it follows that only transitions for which $\Delta M_J=0,\pm 4,\pm 8,\ldots$ are allowed. In the 90° or xx polarisation, four tensor products occur, $C_1^{(1)}C_1^{(1)}$, $C_{-1}^{(1)}C_{-1}^{(1)}$, $C_1^{(1)}C_{-1}^{(1)}$, and $C_{-1}^{(1)}C_1^{(1)}$. The first two of these allow changes in M_J of ± 2 (or ± 6 etc., in combination with the crystal field) while the third and fourth leave it unchanged. In the 45° polarisation, with the field of each photon projected onto the x and z axes, the two-photon field products are $\frac{1}{2}(xx+zz+xz+zx)$. The xz and zx components introduce operator products of the form $C_1^{(1)}C_0^{(1)}$ and $C_{-1}^{(1)}C_0^{(1)}$, which link states with $\Delta M_J=\pm 1$ (or ∓ 3, ± 5, etc.).

These selection rules can be used to calculate the intensity of the Zeeman components of transitions from the $^7F_6(A_{1g})$ ground state of octahedral Tb^{3+} to *gerade* excited state crystal field levels. To lighten the notation the *gerade* state labels will be omitted. The direct product of the electric-dipole operators, $T_1\otimes T_1$, contains $A_1+E+[T_1]+T_2$. In the absence of a magnetic field these are the symmetries of the allowed excited states, with the exception of the T_1 representation which is formed from the anti-symmetric product. The expansion of octahedral states in the $|JM_J\rangle$ basis, when z corresponds to a C_4 axis, is given by Griffith.[18] For integral J, the octahedral basis functions fall into four blocks. The A_1, $T_1(0)$ and $E\theta$ states are expanded from bases with $M_J=0,\pm 4,\pm 8,\ldots$. Similarly A_2, $E\varepsilon$, $T_2(0)$ are derived from $M_J=\pm 2,\pm 6,\ldots$; $T_1(+1)$, $T_2(-1)$from $M_J=+1,-3,+5,\ldots$; and $T_1(-1)$, $T_2(+1)$ from $M_J=-1,+3,-5,\ldots$.

The main features of the polarisation can now be deduced from the M_J selection rules, and are summarised in Table I. Although this table includes $T_2(0)$ excited states, $A_1\rightarrow T_2(0)$transitions in the xx, xz, and zz polarisations are forbidden in first order. This arises from the relative phases of conjugate $|J,M_J\rangle$ and $|J,-M_J\rangle$ pairs in the octahedral states. It can readily be shown, by expanding the $LSJM_J$ basis in an LM_LSM_S basis, that their contributions always differ in phase, so that the intensity vanishes. However in the presence of second order interactions induced by the magnetic field, the coefficients of the conjugate pairs need no longer be equal, and the transitions can become allowed. On the other hand, an $A_1\rightarrow T_2(0)$transition is allowed in the xy polarisation in first order, because

$$xy=\frac{ir^2}{2}[C_{+1}^{(1)}C_{+1}^{(1)}-C_{-1}^{(1)}C_{-1}^{(1)}]$$

and the form of the spherical tensor operators, taken with the opposed phase of the conjugate basis functions, ensures a non-zero transition moment. The results in Table I can also be obtained from the coupling coefficients $\langle T_1 iT_1 j|T_1T_1\Gamma\gamma\rangle$ that define a two-photon transition moment tensor with symmetry $\Gamma\gamma$ in the octahedral group. These are tabulated by Griffith.[18]

TABLE I. Selection rules for M_J, and excited states accessible by TPE from an A_1 ground state in O_h symmetry, as a function of the polarisation.

Polarisation	Field components	Operator	ΔM_J	Excited States
0^0	zz	$C_0^{(1)}C_0^{(1)}$	$0,\pm4$	A_1,Eθ
90^0	xx	$+\frac{1}{2}C_{\pm1}^{(1)}C_{\pm1}^{(1)}$	$\pm2,\pm6$	Eε, $T_2(0)$[a]
		$-\frac{1}{2}C_{\pm1}^{(1)}C_{\mp1}^{(1)}$	$0,\pm4$	A_1,Eθ
45°	$\frac{1}{2}zz$	$\frac{1}{2}C_0^{(1)}C_0^{(1)}$	$0,\pm4$	A_1,Eθ
	$\frac{1}{2}xx$	$\frac{1}{4}C_{\pm1}^{(1)}C_{(\pm1}^{(1)}$	$\pm2,\pm6$	Eε, $T_2(0)$[a]
		$-\frac{1}{4}C_{\pm1}^{(1)}C_{\mp1}^{(1)}$	$0,\pm4$	A_1,Eθ
	xz	$C_0^{(1)}C_{+1}^{(1)}$	$+1,-3,+5$	$T_2(-1)$
		$C_0^{(1)}C_{-1}^{(1)}$	$-1,+3,-5$	$T_2(+1)$

[a]$T_2(0)$ states are only allowed in second order.

B. Angular dependence of the intensity of E and T_2 excited states

The angular dependence of the intensity for components of E excited states is conveniently described using a Cartesian representation of the transition moment tensors. The optical field vectors are projected onto the second rank tensors $T_{E\theta}$ and $T_{E\varepsilon}$, whose normalisation is derived from the spherical harmonics,[18]

$$E\theta = |20\rangle \sim \frac{1}{2}(2z^2 - x^2 - y^2),$$

$$E\varepsilon = \frac{1}{\sqrt{2}}(|22\rangle + |2-2\rangle) \sim \frac{\sqrt{3}}{2}(x^2 - y^2).$$

With the optical field in the xz plane, we may write in the notation of Bader and Gold:[11]

$$\boldsymbol{\varepsilon}.T_{E\theta}.\boldsymbol{\varepsilon} \propto \frac{1}{2}(2n^2 - l^2),$$

$$\boldsymbol{\varepsilon}.T_{E\varepsilon}.\boldsymbol{\varepsilon} \propto \frac{\sqrt{3}}{2}(l^2),$$

where $\boldsymbol{\varepsilon}$ is a unit polarisation vector, defined by direction cosines (l,m,n) with respect to the crystallographic axes x,y,z. The intensity of each transition, $I_{g\to f}$, is proportional to $|\langle g|\boldsymbol{\varepsilon}.\mathbf{T}.\boldsymbol{\varepsilon}|f\rangle|^2$, so that

$$I_{E\theta} \propto \frac{1}{4}(4n^4 - 4n^2l^2 + l^4),$$

$$I_{E\varepsilon} \propto \frac{3}{4}(l^4). \tag{2}$$

Values of these functions at specific angles in the xz plane are given in Table II. Notice that in the absence of a field, when Eε and Eθ are degenerate, their total intensity at 45° is a quarter of that at 0° and 90°, in agreement with the expressions of Bader and Gold.[11]

Figure 1 shows polarised TPE spectra for transitions to the $^5L_{10}(E_a)$ state of Cs_2NaTbF_6 in a 4.5 T field parallel to [001]. Inspection of the eigenfunctions of a Hamiltonian that includes the Zeeman interaction, indicates that the higher energy of the two Zeeman components is dominated by the Eθ basis state. In the 0° polarisation only this component has any intensity, and at 90° this falls by a factor of approximately 4, in accordance with the properties of an Eθ state in Table II. The relative intensities of the lower energy component at 45° and 90° are also close to those predicted for an Eε state. However it is clear that the intensity of the Eε transition at 90° is smaller relative to the Eθ transition at 0°

TABLE II. Relative two-photon absorption intensities from an A_1 ground state in O_h symmetry, as a function of the polarisation in the xz plane.

Polarisation	A_1	Eθ	Eε	$T_2(-1)$	$T_2(0)$	$T_2(+1)$
0°	1	1	0	0	0	0
45°	1	1/16	3/16	1	$y/4$[a]	1
90°	1	1/4	3/4	0	y[a]	0

[a]y is a second-order intensity, dependent upon the magnetic field strength.

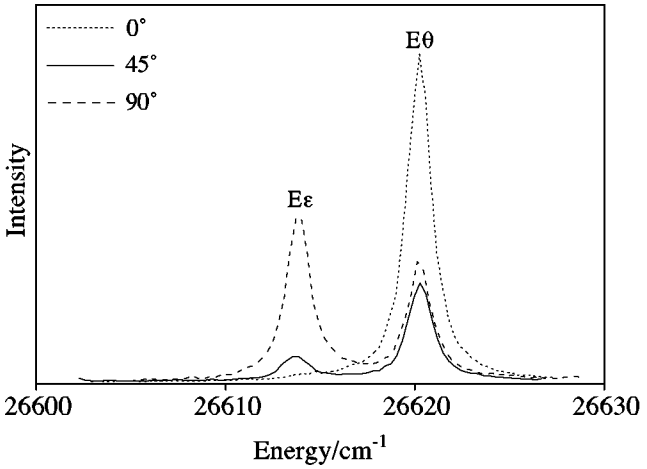

FIG. 1. TPE polarisations of the $^7F_6 \to {}^5L_{10}$ (E_a) transition in Cs_2NaTbF_6 at 4.5 T and 5 K.

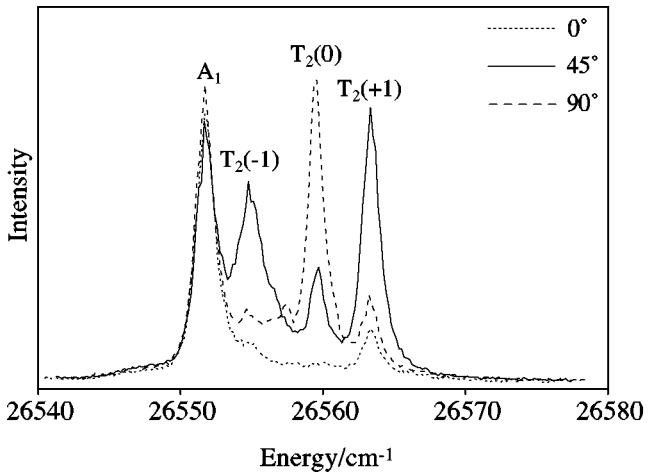

FIG. 2. TPE polarisations of the $^7F_6 \rightarrow {}^5G_6(A_1,T_a)$ transitions in Cs_2NaTbF_6 at 3.0 T and 5 K.

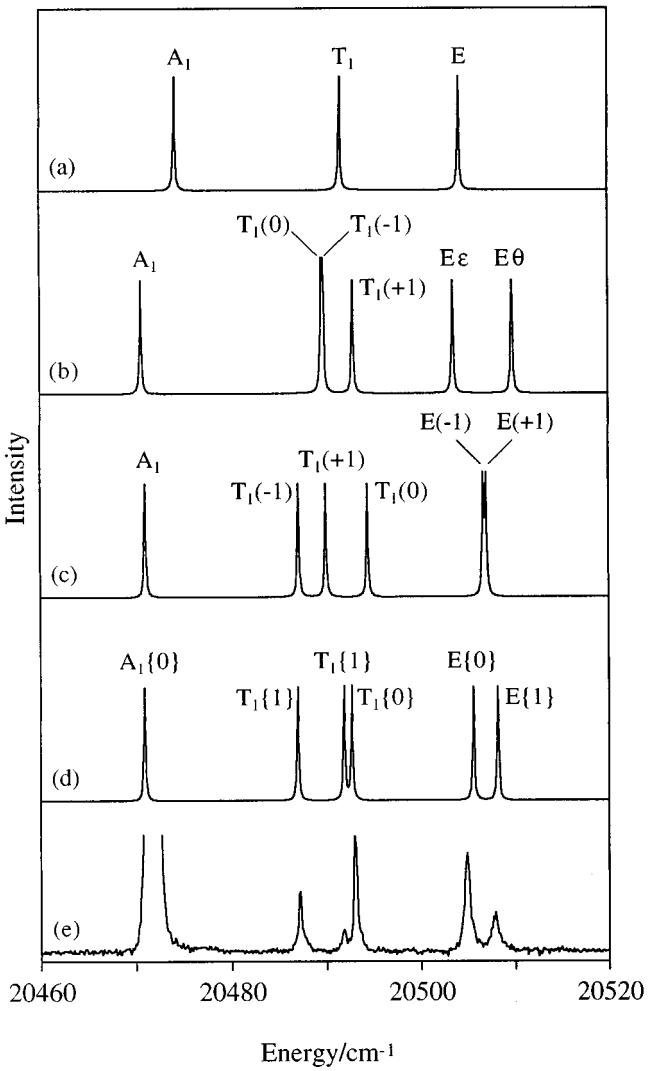

FIG. 3. Calculated energies of the $^5D_4(A_1, T_1, E)$ components in $Cs_2NaTbCl_6$ (a) at zero field, and for a field of 4.5 T along (b) C_4, (c) C_3, and (d) C_2' symmetry axes. The experimental spectrum (e) is shown at 4.5 T. In (b) and (c) the components are labelled as in the text, and in (d) a characteristic M_J value is included in parentheses.

than the expected ratio of 3:4, and that the theory fails to account for the large intensity in the Eθ transition at 45°.

The Eθ, Eε degeneracy cannot be lifted by a first-order perturbation, so we attribute the anomalous intensity ratio to the modified wavefunctions that underly the second-order Zeeman splitting. For example, $T_2(0)$and Eε states can be strongly coupled, because they are derived from the same JM_J bases and the Zeeman interaction is diagonal in M_J. Equivalently, the coupling coefficient of the z component of the Zeeman operator (which transforms as $T_1(0)$ in O_h) with $T_2(0)$, $\langle T_1(0)T_2(0)|T_1T_2E\varepsilon\rangle$, is non-zero.[18] However $A_1 \rightarrow T_2(0)$transitions have no intensity in first order, so the admixture of a $T_2(0)$ with an Eε state lowers the intensity of $A_1 \rightarrow E\varepsilon$ relative to $A_1 \rightarrow E\theta$ transitions, as observed. Other second-order interactions can contribute to such intensity anomalies in a similar way.

For T_2 excited states, it is natural to use a complex basis that is diagonal to first order in the Zeeman interaction, i.e.,[18]

$$T_2(+1) = -\frac{i}{\sqrt{2}}(yz + ixz),$$

$$T_2(0) = ixy,$$

$$T_2(-1) = \frac{i}{\sqrt{2}}(yz - ixz).$$

It is clear that no intensity is expected in the $xx(90^0)$ or $zz(0^0)$ polarizations. With the electric vector in the xz plane, the yz contributions to the transition moments vanish, and the intensity mechanism is the same for both the $T_2(+1)$ and $T_2(-1)$ states. As before we note that transitions to $T_2(0)$are forbidden to first order. In the notation of Bader and Gold,[11]

$$\boldsymbol{\varepsilon}.T_{T_2(0)}.\boldsymbol{\varepsilon} = 0,$$

$$\boldsymbol{\varepsilon}.T_{T_2(+1)}.\boldsymbol{\varepsilon} = \boldsymbol{\varepsilon}.T_{T_2(-1)}.\boldsymbol{\varepsilon} \propto ln.$$

It follows that $A_1 \rightarrow T_2(\pm 1)$ transitions should only appear in the 45° polarisation. In practice we should expect second-order corrections to this simple result. These properties are incorporated in Table II, where the $A_1 \rightarrow T_2(0)$transition is shown to acquire some of the intensity and polarisation characteristics of an $A_1 \rightarrow E\varepsilon$ transition.

Figure 2 illustrates TPE spectra of Cs_2NaTbF_6 in the $^5G_6(A_1,T_{2a})$ region. The A_1 band is clearly independent of polarisation. As expected from Table II, the $A_1 \rightarrow T_2(\pm 1)$ transitions are both strongly polarised at 45°. Second order interactions ensure that the $A_1 \rightarrow T_2(0)$transition can obtain intensity in the 90° polarisation. One such is the interaction of $T_2(0)$with nearby Eε states (the closest, $^5L_{10}(E_a)$, is 55 cm^{-1} away). However the interaction between the A_1 ground state and the first excited $T_1(0)$state, 55 cm^{-1} above it, is of more general importance. It ensures that all $A_1 \rightarrow T_2(0)$ transitions acquire $T_1(0) \rightarrow T_2(0)$ character.

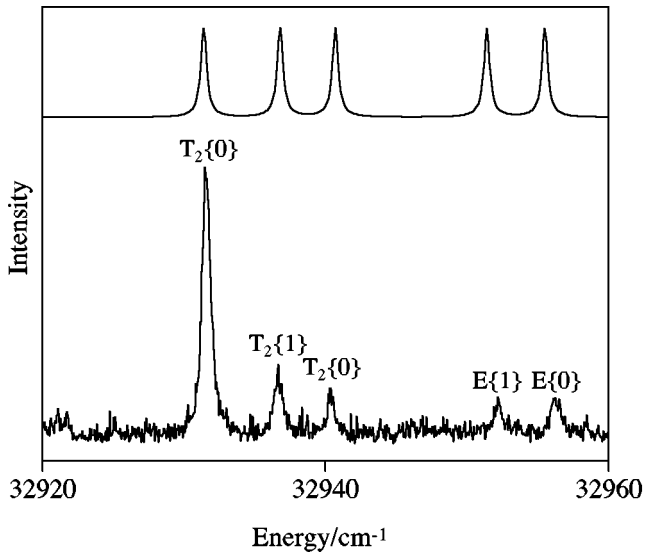

FIG. 4. Calculated and experimental TPE spectra in the $^7F_6 \rightarrow {}^5H_6(T_{2b}, E)$ region of $Cs_2NaTbCl_6$ at 10 K and a field of 4.5 T parallel to [110]. Features are labelled in the convention of Figure 3d.

Since the $\langle T_1(0)E\varepsilon | T_1 E T_2(0)\rangle$ coupling coefficient is non-zero, these transitions also acquire a polarisation characteristic of the Eε transition moment tensor, and are allowed in the 90° polarisation (cf. equation (2)). The $A_1 \rightarrow T_2(0)$ intensity in Figure 2 is reduced by a factor of 4 at 45°, and is absent in the 0° polarisation, as indicated in Table II. The residual intensity in the $A_1 \rightarrow T_2(\pm 1)$ transitions in the 0° and 90° polarisations is not easy to account for and may signal a small misalignment of the crystal axes with respect to the field. This may also be the cause of the anomalous 45° intensity of the Eθ component in Figure 1.

IV. ZEEMAN ENERGIES

A. Anisotropy

The Zeeman anisotropy of ions in cubic crystals has been carefully examined by Yeakel.[19] The Zeeman operator transforms as T_1 in O_h, so for even electron systems *first-order* Zeeman splittings only occur in states of T_1 and T_2 symmetry. Yeakel has shown that these are always isotropic. However there are numerous non-zero matrix elements of the Zeeman operator that are off-diagonal in the irreducible representations of O_h, and these can give rise to anisotropy in the Zeeman energies. Within a lanthanide multiplet, Zeeman energies are often comparable to the crystal field separation of states, so that the consequential anisotropy can be significant.

TPE spectra of $Cs_2NaTbCl_6$ were acquired using depolarised excitation in order to provide access to all Zeeman components. The orientation of the magnetic field relative to the crystal axes was not initially determined, however the Zeeman anisotropy is sufficiently large and characteristic that it was possible to establish that the field direction is close to [110], i.e. a C_2' axis of the octahedron. Figure 3 shows a simulation of the TPE spectrum in the region of the A_1, T_1 and E components of the $^5D_4$ multiplet, for both zero field and a field of 4.5 T along the C_4, C_3, and C_2' axes. The calculation uses the F-Shell code written by M.F. Reid,[20] and a potential expansion appropriate to the choice of z axis, along which the Zeeman field is applied. Although the calculation includes the T_2 component of this multiplet, it is well separated from the A_1, T_1 and E states, and can be ignored for the purposes of the argument that follows. Further, $^5D_4$ is separated by more than 5000 cm^{-1} from its neighbours, so significant Zeeman interactions only occur within the multiplet. The crystal field parameters were chosen to ensure good agreement with the band positions in the absence of the magnetic field. Comparison with the experimental spectrum, which is included in Figure 3, illustrates close agreement with the C_2' simulation, and the failure of the other two models.

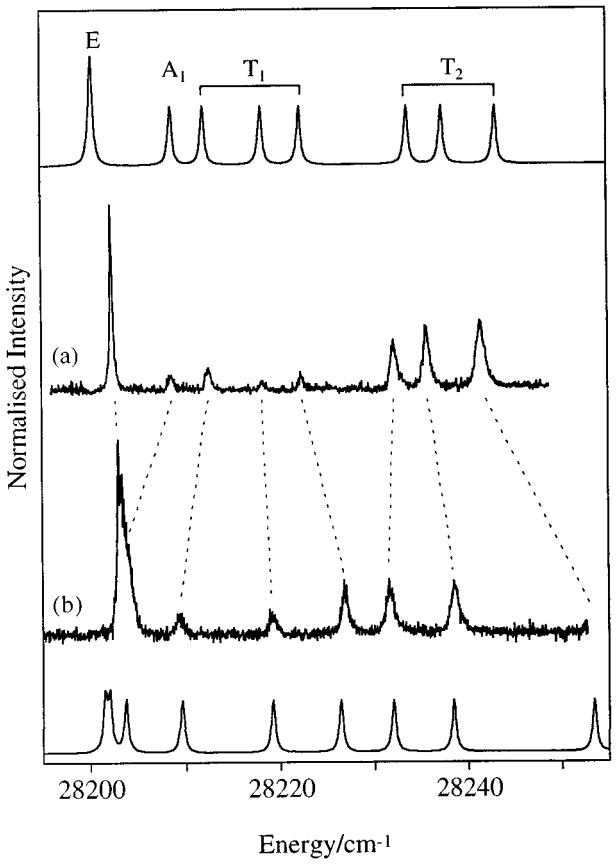

FIG. 5. Calculated and experimental TPE spectra in the $^7F_6 \rightarrow {}^5D_2(E)$, $^5G_4(A_1)$, and $^5L_9(T_{1a}, T_{2a})$ region of $Cs_2NaTbCl_6$ at 10 K, and a field of (a) 2.0 T and (b) 4.5 T parallel to [001].

No attempt was made to compute TPE intensities because, despite recent attempts to analyse the mechanisms that apply to this multiplet, the theory is not yet reliable.[21,22] Instead features of constant intensity with a realistic Gaussian line-shape were used in the simulation. It should be emphasised that the $A_1 \rightarrow T_1$ transitions are forbidden in the absence of the magnetic field, and their intensity is an obvious manifestation of the second-order Zeeman effect.

The origin of the magnetic anisotropy may be qualitatively understood by examining the second-order interac-

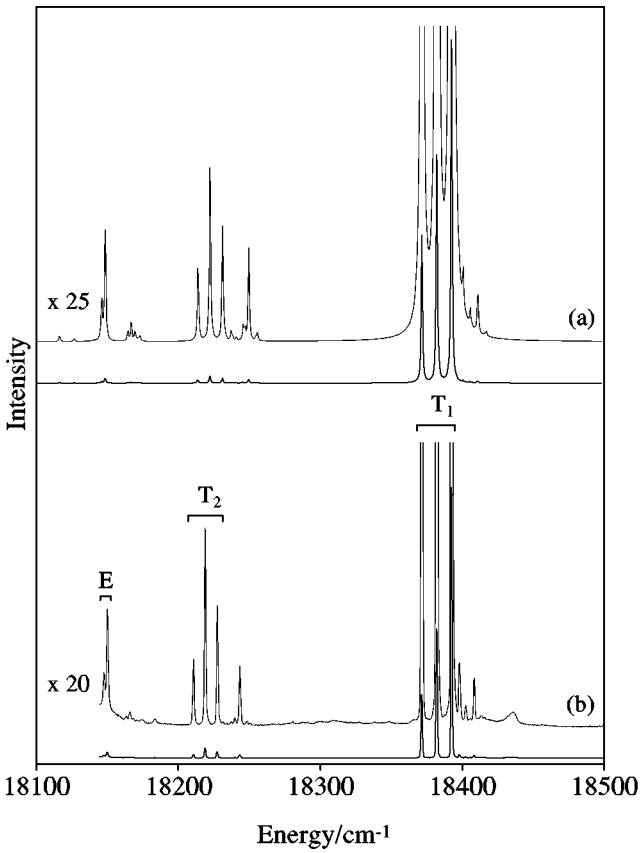

FIG. 6. (a) Calculated and (b) experimental one-photon emission spectra, in the $^5D_4 \rightarrow {}^7F_5$ region of $Cs_2NaTbCl_6$ at 5.0 T and 6 K. Transitions from $^5D_4(A_1)$ are labelled with their final state symmetry; remaining features in the calculated spectrum arise from thermal population of $^5D_4(T_1)$.

tions. Figure 3b shows the Zeeman levels when z is in the C_4 direction. Noting the form of the $|JM_J\rangle$ bases and that the Zeeman interaction is diagonal in M_J, it is apparent that second order interactions only occur between Eθ and the nearby $T_1(0)$ and A_1 states. Eε therefore remains unperturbed, while the $T_1(\pm 1)$ components are split by a first order Zeeman effect. The result is a large separation of the E components and the near degeneracy of the $T_1(0)$ and $T_1(-1)$ components near 20 490 cm^{-1}. Notice that the downwards shift of the $T_1(0)$component is quite small, because it interacts with both the A_1 state to lower energy and the Eθ state to higher energy.

A trigonal basis is convenient if the field is parallel to a C_3 axis (Figure 3c). The A_1 and $T_1(0)$ states are then derived from basis functions with $M_J = 0, \pm 3$; E(1), $T_1(+1)$ from the set with $M_J = 4,1,-2$; and E(-1), $T_1(-1)$from $M_J = 2,-1,-4$. In this basis $T_1(0)$ does not interact with the E states and is influenced only by the A_1 state to lower energy. It is therefore displaced to the high energy side of the other T_1 components, and occurs near 20 493 cm^{-1}. The E states near 20 506 cm^{-1} now have identical off-diagonal matrix elements linking them to the $T_1(\pm 1)$ states, so they retain their intrinsic degeneracy, with the exception of a small second-order effect that reflects the first order $T_1(\pm 1)$ splitting. Notice that the centre of gravity of the $T_1(\pm 1)$ states is shifted down by about 3 cm^{-1} relative to its location in the C_4 orientation (i.e., the zero field energy), by interaction with the E states, which in turn shift by an equal interval to higher energy relative to the position of the unperturbed Eε state in the C_4 model.

Finally, when the field is applied along a C_2' axis the eigenfunctions separate into two blocks, distinguished by whether the basis functions are comprised of states with even or odd M_J. All the components are now subject to second order interactions within each block, and the pattern of energies is in excellent agreement with experiment.

B. Application to selected multiplet components

The high density of excited states poses severe difficulties for the correct assignment of individual levels. For example in Cs_2NaTbF_6 we have been able to locate 80 excited states in the 9000 cm^{-1} interval between 26 000 and 35 000 cm^{-1}. In some regions the components of several multiplets overlap. Indeed, near 28 500 cm^{-1}, the average separation of a set of 9 levels is only 24 cm^{-1}. Although the correct assignments can often be assisted by empirical energy level calculations,[4] residual ambiguities arise from the failure of the one-electron crystal field Hamiltonian, and ignorance of the correlation crystal field (CCF) parameters. The CCF can cause the crystal field splitting of a number of multiplets to deviate dramatically from the predictions of the one-electron model.[10] Additional data are therefore vital in assigning the correct multiplet parentage to individual levels.

When second order Zeeman interactions are small it is often possible to use experimental g-values to distinguish between excited states of the same symmetry. We have recently reported an example for the $^5D_2(T_2)$ and $^5L_9(T_{2a})$ states, in the spectrum of Cs_2NaTbF_6.[23] In the absence of the magnetic field these states are only separated by 5 cm^{-1}, but the difference in their g-values makes their assignment unambiguous. However in the majority of multiplets it is essential to test the assignment by a full calculation of the Zeeman perturbation. Because of the limitations of the one-electron crystal field, it is necessary to adjust the empirical parameters in the Hamiltonian so as to accurately describe the zero-field energies in each region of interest, before computing the Zeeman spectrum. When this is done the spectrum can usually be modelled to within a few wavenumbers.

An example of this approach is shown in part of the isolated $^5H_6$ multiplet of $Cs_2NaTbCl_6$. By varying the crystal field, the zero field energy levels were fit almost exactly, and the resulting Zeeman energies are in excellent agreement with experiment (Figure 4). By contrast the region shown in Figure 5 comprises peaks from the $^5D_2$, $^5G_4$, and $^5L_9$ multiplets. This figure shows that it is possible to model a complex set of first and second order interactions, as well as substantial changes in the pattern of levels that develop as the field increases. Less than perfect agreement between experiment and simulation, in some parts of this spectrum, is attributable to our inability to find an ideal parameterisation of the zero-field spectrum within the one-electron crystal field approximation.

Finally we illustrate the quality of the wavefunctions by simulating the magnetic-dipole intensity in the *one-photon* Zeeman spectrum of the $^5D_4 \rightarrow {}^7F_5$ transition of $Cs_2NaTbCl_6$, at a temperature of 6 K (Figure 6). Almost every feature of the experimental spectrum is reproduced with a high degree of fidelity. In this way, we have been able to model eleven regions of the emission spectrum corresponding to the $^5D_{4,3} \rightarrow {}^7F_{6,5,4,3,2,1}$ transitions. Our study of the TPE spectrum of $Cs_2NaTbCl_6$ includes 22 excited multiplet regions extending up to 40 000 cm^{-1}, for which the assignments have been clarified by the Zeeman data.

A full set of energy level assignments for $Cs_2NaTbCl_6$ and Cs_2NaTbF_6, strengthened by the Zeeman analysis outlined above, will be described in a forthcoming paper.[24]

ACKNOWLEDGMENTS

We thank the Association of Commonwealth Universities for the award of a Commonwealth Scholarship to A.J.B. and the EPSRC for the support of I.D.M. We are also most grateful to M.F. Reid for the use of his F-Shell program, and R.C.C. Ward and A. Egesel for the growth of the fluoride elpasolite crystal.

[1] L. R. Morss, M. Siegal, L. Stenger, and N. Edelstein, Inorg. Chem. **9**, 1771 (1970).
[2] B. R. Judd, J. Chem. Phys. **66**, 3163 (1977).
[3] M. F. Reid, J. Chem. Phys. **87**, 2875 (1987).
[4] M. F. Reid and F. S. Richardson, J. Chem. Phys. **83**, 3831 (1985).
[5] P. A. Tanner, V. V. Ravi Kanth Kumar, C. K. Jayasankar, and M. F. Reid, J. Alloy Comp. **215**, 349 (1994).
[6] G. H. Dieke, *Spectra and Energy Levels of Rare Earth Ions in Crystals* (Wiley, New York, 1968).
[7] W. T. Carnall, G. L. Goodman, K. Rajnak, and R. S. Rana, J. Chem. Phys. **90**, 3443 (1989).
[8] R. G. Denning, Eur. J. Solid State Inorg. Chem. **28**, 33 (1991).
[9] M. Bouazaoui, B. Jacquier, C. Linares, and W. Strek, J. Phys. Condensed Matter **3**, 921 (1991).
[10] A. J. Berry, C. S. McCaw, I. D. Morrison, and R. G. Denning, J. Lumin. **66/67**, 272 (1996).
[11] T. R. Bader and A. Gold, Phys. Rev. **171**, 997 (1968).
[12] B. Jacquier, J. C. Gacon, J. F. Marcerou, M. F. Joubert, and R. L. Cone, J. Lumin. **40/41**, 517 (1988).
[13] G. K. Liu, W. T. Carnall, R. P. Jones, R. L. Cone, and J. Huang, J. Alloy Comp. **207/208**, 69 (1994).
[14] J. Huang, G. K. Liu, and R. L. Cone, Phys. Rev. B **39**, 6348 (1989).
[15] B. Jacquier, J. C. Gacon, Y. Salem, C. Linares, and R. L. Cone, J. Phys. Condensed Matter **1**, 7385 (1989).
[16] B. R. Judd, *Operator Techniques in Atomic Spectroscopy* (McGraw–Hill, New York, 1963).
[17] M. C. Downer, *Topics in Applied Physics*, edited by W. M. Yen (Springer, Berlin, 1989), Vol. 65, p. 29.
[18] J. S. Griffith, *The Theory of Transition-Metal Ions* (Cambridge University Press, London, 1961).
[19] W. C. Yeakel, Mol. Phys. **33**, 1429 (1977).
[20] M. F. Reid (private communication).
[21] A. Ceulemans and G. M. Vandenberghe, Phys. Rev. B **53**, 8310 (1996).
[22] M. Chua and P. A. Tanner, Phys. Rev. B **54**, 11014 (1996).
[23] A. J. Berry, R. G. Denning, and I. D. Morrison, Chem. Phys. Lett. **266**, 195 (1997).
[24] A. J. Berry, I. D. Morrison, and R. G. Denning (in preparation).